LANGMUIR

pubs.acs.org/Langmuir Article

Impact of Bulk Nanobubble Water on a TiO_2 Solid Surface: A Case Study for Medical Implants

Masayoshi Takahashi,* Masahiro Nakazawa, Takahiro Nishimoto, Mitsuyuki Odajima, Yasuyuki Shirai, and Shigetoshi Sugawa

Cite This: https://doi.org/10.1021/acs.langmuir.4c03339 Read Online

ACCESS | Metrics & More | Article Recommendations | Supporting Information

ABSTRACT: In the field of medical implants, enhancing the wettability of artificial surfaces is crucial for improving biocompatibility. This study investigates the potential of ozone nanobubble water, an aqueous solution known for its strong oxidizing and sterilizing properties, to modify the surface of titanium dental implants. By immersing the implants in ozone nanobubble water for ∼10 min, we observed a significant transformation of their surface characteristics. Implant surfaces that had become hydrophobic over time, likely due to organic contaminants, became superhydrophilic, exhibiting a contact angle near zero. Fresh implant material is initially hydrophilic but becomes hydrophobic within a few days of drying. In sharp contrast, the hydrophilicity induced by ozone nanobubble water treatment persisted for more than one month. This durability suggests not only the removal of organic matter through cleaning but also a substantial alteration in the surface properties of the implants. The generation of ozone nanobubble water involved releasing ozone microbubbles into an aqueous solution containing trace amounts of iron and manganese, resulting in spherical particles with an average diameter of ∼10 nm. These particles could be bulk nanobubbles, a stabilized gas body surrounded by a solid shell composed of iron hydroxide. Termed "nanoshells" in our previous study, these particles demonstrated exceptional dispersibility without the need for stabilizing agents such as surfactants or capping agents, attributed to their inherent high wettability. The sustained hydrophilicity of the implant surfaces might be attributed to the adherence of these hydrophilic nanoshells to the implant's surface. This study highlights the potential of ozone nanobubble water for long-term surface modification of dental implants, offering a promising avenue for enhancing implant biocompatibility.

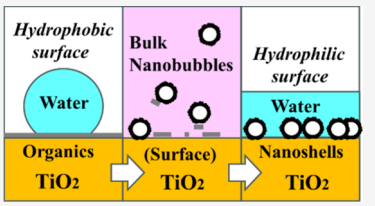

1. INTRODUCTION

Bulk nanobubbles have been attracting considerable attention for their potential applications across a broad spectrum of scientific and technological fields. Investigating how bulk nanobubbles modify the surface properties of solid materials is believed to hold significant promise for various technological applications. However, this area remains largely unexplored, especially regarding its impact on the wettability of metallic materials. Improving surface wettability is vital for numerous applications, prompting extensive research in this domain.[1−12] Given the extensive studies already conducted on the surface properties of metallic materials, they represent a significant target for further research involving nanobubbles. Wettability of metal surfaces is known to be sensitive to both chemical composition and surface structure, the latter being significant even at the level of lattice structure. For instance, the contrasting wettability between the hydrophobic Cu(111) surface and the hydrophilic Cu(110) can be linked to the arrangement and state of surface water molecules. The former is characterized by a closely packed hexagonal arrangement that presents fewer active sites for water molecule adsorption, whereas the latter, with its more open rectangular atomic arrangement, increases the surface reactivity, leading to enhanced wettability and hydrophilic behavior. Lattice defects and surface terminations also play a crucial role in determining the hydrophilicity of metal surfaces. Furthermore, oxidation, a common process for most minerals under environmental conditions, significantly alters surface wettability. The presence of oxygen, in the form of surface oxides acting as Lewis bases with available electron pairs, can markedly influence the hydrogen bonding network of water molecules at the interface, thereby affecting the surface wettability.[13,14] Moreover, surface contamination can drastically change wettability. Oxygen-containing functional groups (such as hydroxyl, −OH) on surfaces can form bonds with hydrogen atoms in water molecules, facilitating hydrogen bonding. Additionally, organic contaminants significantly affect wettability by obscuring the material's intrinsic surface properties, often making it more hydrophobic. Understanding these factors is crucial for the development of materials with engineered surface properties for enhanced technological applications.

It is increasingly evident that tiny bubbles, including microbubbles and nanobubbles, can endow aqueous solutions

Received: August 24, 2024
Revised: November 12, 2024
Accepted: November 13, 2024

with various functions.[15−28] These capabilities extend to solid surfaces as well. Notably, ozone microbubbles have been demonstrated to facilitate the rapid removal of photoresist from silicon wafers, an advancement that promises significant potential for semiconductor manufacturing.[29] This function is attributed to the interaction between the gas−water interface and the solid surface, further characterized by the generation of hydroxyl radicals, a feature not present in ordinary ozone water.[30−33] In addition to cleaning semiconductor wafers, these tiny bubbles could enhance the properties of solid surfaces. Meanwhile, nanobubbles, might be defined by their diameter of less than 50 nm and their long-term stability, are anticipated to have effects distinct from microbubbles. While the shrinking gas−water interface of collapsing microbubbles contributes to their mechanisms of action, the stability and exceedingly small size of nanobubbles might be critical for their applications.

Numerous methods for generating nanobubbles have been proposed, each likely to confer distinct properties on the nanobubbles depending on the technique used. We employed a method based on microbubbles, which are well-known for their characteristics.[15,16,34,35] Microbubbles, defined as tiny bubbles less than 50 μm in diameter, can be produced using commercially available microbubble generators, such as those employing pressurized dissolution. Microbubbles possess two key properties that promote the formation of nanobubbles: rapid underwater shrinkage and an electrically charged gas−water interface. The rapid shrinkage, leading to the microbubble collapse, is attributed to their high surface-to-volume ratio and the pressurized condition inside the bubble caused by surface tension, which leads to swift gas dissolution.[36] The charged interface results from the adsorption of aqueous ions, specifically protons (H^+) and hydroxide ions (OH^-), which accumulate during the process of microbubble collapse.[16,37,38] To enhance the stability of the generated nanobubbles, we introduce iron ions and ozone gas into the aqueous solution.[34,35] Ferrous ions are added first, followed by the introduction of ozone gas to create ozone microbubbles. As these microbubbles collapse, the gas−water interface becomes a specialized reaction field, facilitating the formation of a solid shell. The accumulated iron ions oxidize and react with hydroxide ions, leading to the formation of iron hydroxide or iron oxides. This process results in the stabilization of collapsing microbubbles as bulk nanobubbles encased in the solid shell, often referred to as "nanoshells", which prevents gas dissolution. Our previous research has shown that these generated nanobubbles possess a distinctive ability to produce hydroxyl radicals (·OH), dispersing accumulated energy as chemical potential when a strong acid, such as HCl, is added to the aqueous solution.[34] This capability may induce specific properties in nanobubble water, potentially modifying the surface characteristics of solid materials.

Transition metals, distinct in their fundamental properties from silicon—the foundation of electronic circuits—possess unique functionalities. Among these metals, titanium is particularly notable for its strength, stability, and exceptional biocompatibility, making it a promising candidate for various biomaterial applications.[7,8,39,40] This is especially true in the context of dental implants, designed to replace missing teeth, where the surface characteristics of the metal play a crucial role. Merely placing the implant in the gum tissue is not sufficient; achieving osseointegration, which is the process of bone growing tightly around the implant to ensure its integration with the bone, is essential to improve chewing function. Such integration necessitates a hydrophilic implant surface, enhanced biocompatibility through mechanisms such as improved blood flow. Hydrophilicity is a key aspect of surface properties, and techniques like sandblasted, large-grit, and acid-etched (SLA) treatment are employed to ensure this characteristic during implantation. Nevertheless, the potential for organic contamination to diminish surface hydrophilicity poses a challenge. Addressing this, our study explores the potential of using bulk nanobubble water to modify the surface of titanium dioxide, a material commonly used in implants, offering a simple yet effective method for altering surface properties in the preoperative stage.

2. MATERIALS AND METHODS

2.1. Titanium Disk Sample. Grade 4 titanium (Ti) disks, conforming to ASTM F67 and ISO 5832−2 standards, with a diameter of 15.0 mm and a thickness of 1.0 mm, were used in this study. The surface of the Ti disks was rapidly oxidized under atmospheric conditions, forming titanium oxide (TiO_2). The disks were specifically prepared with a microroughened surface to promote osseointegration, a critical factor in the success of dental implants. The SLA treatment consisted of a two-step process: first, the disks were sandblasted with large grit aluminum oxide particles to create a textured surface, followed by acid etching in a mixture of hydrochloric and sulfuric acids.[7,8,12] Since the TiO_2 surface of the Ti disks was superhydrophilic after the SLA treatment, the samples were placed in polypropylene containers (29 mm inner diameter, 45 mm height) and left in a room without a lid for 30 days to induce surface hydrophobization. For most experiments, these hydrophobized disks were used as the primary samples; however, fresh, nonhydrophobized Ti disks were also used for comparison purposes.

2.2. Preparation of Ozone Nanobubble Water. The sample preparation followed the protocols established in the previous studies.[34,35,41,42] A decompression type of microbubble generator (A01N; Dan-Takuma Co., Ltd.) circulated water within a 5 L plastic container. Ozone gas, at a concentration of approximately 2% by volume (~50 g/N m^3), with the remainder being pure oxygen, was injected at a rate of 0.5 L/min into the circulating water on the pump's suction side. The generator operated for 30 min, maintaining the water temperature below 25 °C. Ultrapure water (approximately 18 MΩ·cm), enriched with 1 μmol/L $FeSO_4$ and 50 μmol/L $MnSO_4$, was used. $FeSO_4$ aided in stabilizing the bulk nanobubbles, a fact confirmed by AFM observations identifying nanoshells with surface protrusions.[35] $MnSO_4$, while not significantly affecting nanoshell generation, contributed to the formation of permanganate ions (MnO_4^-) in the surrounding aqueous solution due to the oxidative action of the ozone microbubbles. Following the microbubble treatment, the solution was left to settle for a day in the container, then filtered through a 450 nm membrane (MF-Millipore, mixed cellulose esters, HAWP04700) and the samples were stored in dark, at room temperature in plastic bottles for at least 1 month prior to treatments.

Ozone nanobubbles are widely recognized not only for their strong antibacterial properties but also for their remarkably low levels of cytotoxicity, making them an intriguing subject for further application.[16,43,44] Given their proven oxidizing capabilities, there arises a potential for the nanobubble waters to be applied in cleaning processes as well. This study has been initiated with the intention of exploring this potential more deeply. Specifically, it focuses on the anticipated synergistic effect that could arise from combining the oxidizing potential inherent to permanganate ions with the unique properties of nanoshells.

2.3. Wettability Evaluation. Samples of hydrophobized Ti disks were immersed in ozone nanobubble water for 10 min at ambient conditions in a 100 mL beaker containing approximately 80 mL of the solution. Subsequently, the disks were cleansed with deionized water, dried with an air blower. Wettability was evaluated using two methods: observing the dispersion of approximately 30 μL of

https://doi.org/10.1021/acs.langmuir.4c03339
Langmuir XXXX, XXX, XXX−XXX

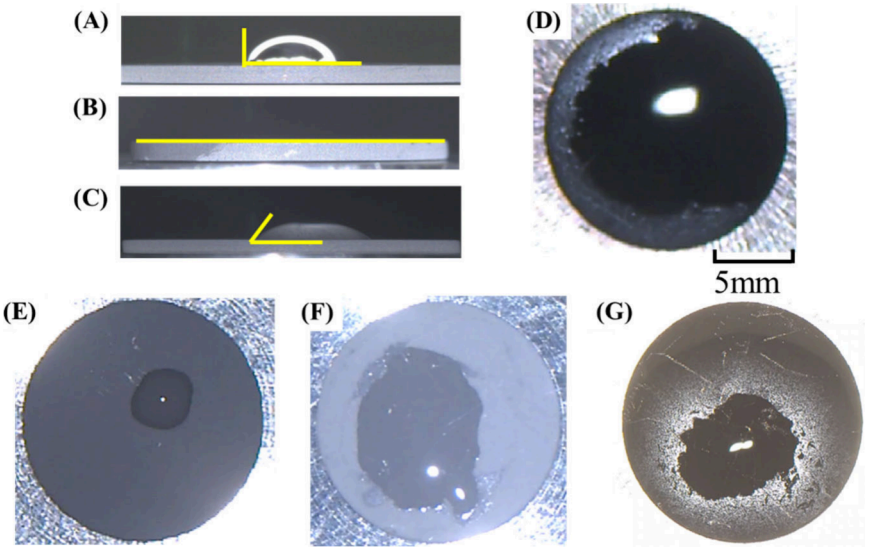

Figure 1. Observations of the dispersion of water dropped on a Ti disk. The photographs were taken after deionized water was dropped in the center of the disk. Images A−C were taken from the side. Images D−G were taken from the top view 5 s after dropping 30 μL of deionized water. Panel A shows the untreated Ti disk as the control sample. Panels B, D, and G show the results after ozone nanobubble treatment. Panels C and E show the results after treatment with $KMnO_4$ water. Panel F shows the result after treatment with deteriorated ozone nanobubble water. For the preparation of the tests, the disk was dipped in the sample water for 10 min and then dried. Images B−F are the results of tests conducted 1 h after the treatments, and panel G is an image from a test conducted 35 days after the treatment. The contact angles of panels A−C were ∼90°, ∼0°, and ∼60°, respectively.

deionized water dropped on the center of the disk via video, and measuring the contact angle of a 2 μL water droplet from the side.[8,12] After measuring hydrophilicity, the sample was dried again with the air blower and then placed in an open polypropylene container to maintain its dry state. This setup allows for periodic reassessment to observe any temporal changes.

3. RESULTS AND DISCUSSION

In this study, we investigated the changes in surface wettability of dental implant materials (Ti disks). Initially, these materials were hydrophobic, as shown in Figure 1-A, with a contact angle of approximately 90°. However, after immersing the samples in ozone nanobubble water for 10 min, their surfaces became hydrophilic. As shown in Figure 1-B, the contact angle significantly decreased to around 0°. Figure 1-D and Video S1 illustrate that water droplets placed on a dry disk rapidly spread and wetted the entire surface in about 6 s.

Organic contamination has been identified as a primary cause of the hydrophobization of titanium dioxide surfaces, particularly in implant materials.[5−8] Given this, the superhydrophilicity observed in implant materials after immersion in ozone nanobubble water is likely due to the effective cleaning of the surface. To explore this further, we extended the immersion time to 24 h and assessed the hydrophilicity of the samples. The results showed no significant change in surface hydrophilicity (see Table 1), indicating that a short immersion time of approximately 10 min in ozone nanobubble water is sufficient to achieve effective surface cleaning.

Implant materials that have been cleaned and rendered hydrophilic can become hydrophobic again depending on storage conditions and surface properties. Considering practical dental applications, changes in surface properties over time are critical. Therefore, we investigated the time-dependent changes in the surface wettability of Ti disks after immersion in ozone nanobubble water for 10 min, under atmospheric conditions. The results, shown in Table 2, indicate that although the surface condition gradually changed over time, the TiO_2 surface maintained its superhydrophilicity even after 35 days (see Video S2). In contrast, the TiO_2 surface of the fresh Ti disk became hydrophobic within 7 days. Despite being stored under similar conditions, these differences raise important questions about the long-term stability of surface treatments. Understanding the time-dependent changes in surface wettability is crucial for assessing the suitability of this technology in dental applications. Further investigation into the underlying mechanisms was therefore conducted.

Table 1. Effects of Treatment on the Wettability of Ti Disks and Changes in Wettability with Treatment Time[a]

	10 min	60 min	24 h
O_3NB	O (96%)	–	O (100%)
$KMnO_4$ water	N (7%)	N (17%)	N (44%)
deteriorated O_3NB	N (41%)	O (80%)	O (100%)

[a]The wettability for each treatment was evaluated on the basis of whether deionized water droplets covered the entire surface of the disk. O indicates that the water covered the entire surface with a contact angle of ∼0°, while N indicates that the water failed to cover the entire surface. To quantitatively assess wettability, the wetted area 5 s after the drop was applied is shown in parentheses as a percentage.

For comparative analysis, we conducted an ultraviolet (UV) irradiation test. A sample with a hydrophobic surface was exposed to UV light for 15 min using a UV-C device (ASM401N; Asumi Giken Co., Ltd.). Immediately after UV irradiation, as shown in Table 2, the implant material exhibited superhydrophilicity and maintained this property for 35 days.

TiO_2 is well-known for its photocatalytic function when exposed to UV light, and this mechanism has been extensively studied. As shown in Figure 2, UV light generates electrons and holes within the TiO_2 material. These charge carriers migrate to the surface and react with oxygen and water molecules, producing reactive species such as hydroxyl radicals (•OH), which effectively decompose organic contaminants.

https://doi.org/10.1021/acs.langmuir.4c03339
Langmuir XXXX, XXX, XXX−XXX

Table 2. Time-Dependent Changes in the Hydrophilicity of Ti Disks under Dry Conditions in an Open Container Exposed to the Atmosphere[a]

	0 days	1 day	7 days	12 days	14 days	35 days
fresh Ti disk	O (98%)	O (59%)	N (7%)	–	–	N (4%)
O_3NB 10 min treatment	O (96%)	–	O (92%)	–	O (88%)	O (85%)
15 min UV-C treatment	O (100%)	–	–	O (90%)	–	O (85%)

[a]The table compares fresh Ti disks, test samples treated with ozone nanobubble water for 10 min, and those treated with UV-C irradiation for 15 min. The wettability of each treatment was evaluated on selected days over a period of 35 days.

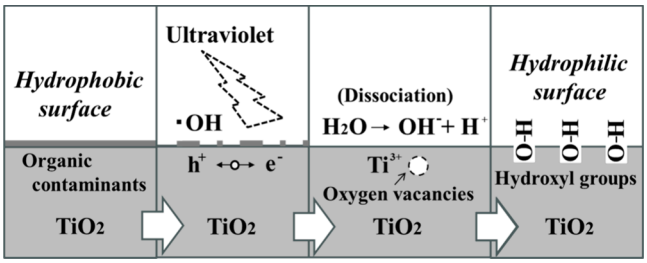

Figure 2. Hydrophilization of the TiO_2 surface of Ti disks by UV irradiation. Upon exposure to UV-C light, the photocatalytic properties of titanium dioxide generate electrons and holes within the material. These charge carriers migrate to the surface, where they produce reactive species that decompose and remove organic contaminants. Concurrently, some Ti^{4+} atoms are reduced to Ti^{3+} while oxygen atoms are oxidized, creating oxygen vacancies. These Ti^{3+} sites and oxygen vacancies facilitate the dissociation of water molecules on the surface, leading to the formation of hydroxyl groups. This process ultimately renders the surface superhydrophilic.

Additionally, some Ti^{4+} near the surface are reduced, while oxygen atoms are oxidized, leading to the formation of Ti^{3+} and oxygen vacancies. These vacancies facilitate the dissociation of water molecules into OH^- ions and protons, which then react with the TiO_2 surface to form hydroxyl groups. The formation of OH groups establishes a hydrogen bond network with water molecules, resulting in enhanced hydrophilicity.

The results of UV irradiation suggest that the sustained hydrophilicity of the TiO_2 surface may be closely linked to the presence of hydroxyl groups. Given their fundamental role in surface wettability, surface functionalization could be a significant factor in the effects observed with ozone nanobubble treatment. Therefore, it may be beneficial to investigate the underlying properties of ozone nanobubble water.

The ESR analysis is one of the most effective methods to clarify the properties of nanobubble waters. However, for the present ozone nanobubble water, the ESR spin-trap method was not appropriate due to the presence of permanganate ions in the aqueous solution. Figure S1 shows the result of UV−vis spectroscopy (V-750; JASCO Corporation) of the ozone nanobubble water, indicating a characteristic absorption peak corresponding to permanganate ions (MnO_4^-). This suggests that the manganese ions introduced during the preparation process were oxidized to form permanganate ions during the ozone microbubble treatment.

Permanganate ions can directly react with the spin-trap reagent 5,5-dimethyl-1-pyrroline N-oxide (DMPO), generating a significant DMPO−OH peak through a nucleophilic reaction. Since the purpose of ESR analysis is to detect free-radical generation, we attempted to remove the permanganate ions from the ozone nanobubble water by using ultraviolet radiation, which is known to decompose permanganate ions. We exposed the ozone nanobubble water to UV-A light (SUV-16; AS ONE Co., Ltd.) for approximately 24 h. After the treatment, the resulting precipitates were removed using a 450 nm membrane filter. Subsequent UV−vis spectrophotometric analysis confirmed the disappearance of the permanganate ion spectrum. This treated water is referred to as "degraded ozone nanobubble water" in this study.

Figure 3 shows the spectrum from the spin-trap ESR observation of the degraded ozone nanobubble water. The

Figure 3. ESR spectrum of the degraded ozone nanobubble water. The spectrum exhibited four distinct peaks with intensity ratios of 1:2:2:1, positioned between those of the Mn^{2+} reference standard. The hyperfine splitting constants were $A_N = A_H = 14.9$ G, indicating the formation of a DMPO−OH adduct.

observation was conducted using the same method as in our previous study.[34] A significant DMPO−OH signal was generated when 100 mM hydrochloric acid (HCl) was added to a mixture of the aqueous solution, 50 mM ethylenediaminetetraacetic acid (EDTA), and 300 mM DMPO. EDTA was used to prevent the nucleophilic attack of H_2O on the spin trap reagent, which was induced by metal ions. Since we also observed a dramatic reduction in peak height with the addition of hydroxyl radical scavengers such as ethanol (see Figure S2), the aqueous solution is likely generating hydroxyl radicals, presumably due to the presence of nanoshells in the solution.

Using the degraded ozone nanobubble water and MnO_4^- aqueous solution, we conducted similar tests with Ti disks that had hydrophobic TiO_2 surfaces. The MnO_4^- solution was prepared by dissolving $KMnO_4$ in distilled water, with the concentration adjusted to match that of the ozone nanobubble water as determined by UV−vis spectroscopy. The Ti disks were then immersed in these two solutions, and their surface hydrophilicity was evaluated, as shown in Table 1. After 10 min of immersion, neither solution induced superhydrophilicity; however, the degraded ozone nanobubble water was more effective than the MnO_4^- solution (see Videos S3 and S4).

https://doi.org/10.1021/acs.langmuir.4c03339
Langmuir XXXX, XXX, XXX−XXX

Extending the immersion time to 60 min and 24 h revealed that the degraded ozone nanobubble water induced superhydrophilicity. In contrast, while the MnO_4^- solution induced some degree of hydrophilicity, it did not achieve superhydrophilicity even after 24 h of treatment.

Although permanganate ions are strong oxidizing agents, they were unable to induce superhydrophilicity in the samples. In contrast, degraded ozone nanobubbles successfully induced superhydrophilicity within a specific time frame. This raises the question: does degraded ozone nanobubble water possess sufficient oxidizing power to decompose organic matter? To investigate this, we conducted ESR spin-trap observations without the addition of HCl to the degraded ozone nanobubble water. The results revealed no significant peaks in the ESR spectrum, indicating that under the conditions in which titanium dioxide is immersed, the degraded ozone nanobubble water does not exhibit significant oxidizing properties.

In the case of actual ozone nanobubbles, where permanganate ions coexist with degraded ozone nanobubble water, a synergistic effect may accelerate the removal of organic contaminants, leading to a rapid transition to a hydrophilic surface. However, these results indicate that oxidation ability does not play a significant role in the surface functionalization leading to the sustained superhydrophilicity of the TiO_2 surface.[45,46]

A possible explanation may be derived from atomic force microscopy (AFM) images of the nanobubble solution.[35] Figure 4 shows the results of AFM observation of nanobubble

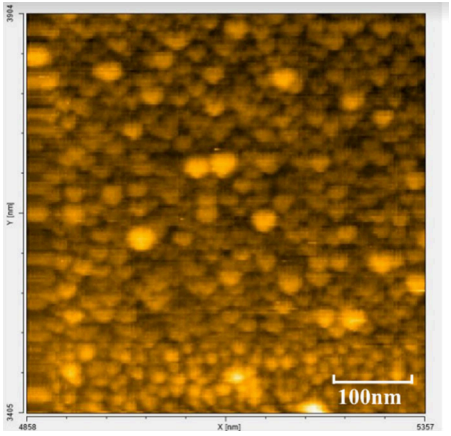

Figure 4. AFM observation of bulk nanobubbles located on a mica substrate treated with 3-(aminopropyl)triethoxysilane. Numerous spherical particles (nanoshells) of <20 nm were observed. Due to the tip size effect in AFM, the nanoshells may appear larger in the surface profile than their actual size.

water generated using the same method as in the present study, but without the addition of manganate ions. The intermittent contact mode AFM (high-speed AFM; Research Institute of Biomolecule Metrology) was used to observe the aqueous solution. A considerable amount of nanoshells were deposited on the positively charged mica substrate treated with 3-aminopropyltriethoxysilane (APTES). It has been demonstrated that these nanoshells possess superhydrophilic properties, contributing to their sustained dispersion for more than six months in the aqueous solution without the need for stabilizing chemicals such as capping agents or surfactants.[34,35]

Figure 5 illustrates a plausible process by which ozone nanobubble water modifies the surface properties of the TiO_2

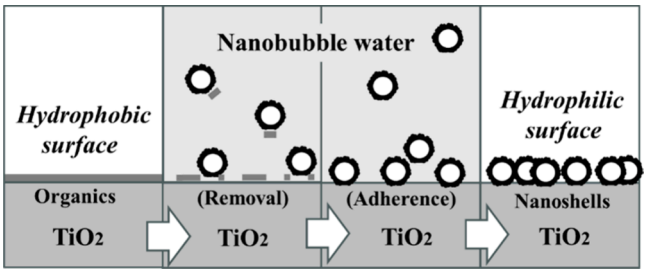

Figure 5. Hydrophilization of the TiO_2 surface of Ti disks by ozone nanobubble water. During the immersion process, nanoshells remove organic contaminants from the surface and adhere to it in large quantities. Due to their superhydrophilic properties, these nanoshells ultimately render the surface superhydrophilic.

surface. Nanoshells may remove organic contaminants from the surface and adhere to it. Since the nanoshells mainly consist of iron hydroxide ($Fe(OH)_3$), which imparts hydrophilic properties through hydroxide groups, the TiO_2 surface covered by these nanoshells could achieve sustained superhydrophilicity. The nanoshells, being less than 20 nm in size with a nanostructured surface, are likely to enhance the surface hydrophilicity due to their high surface energy, similar to the effects observed with lattice defects and surface termination. In addition to the hydroxide groups, the small-scale surface structure of the nanoshells may also contribute to the enhanced hydrophilicity.[47]

4. CONCLUSION

The superhydrophilization of titanium dioxide materials through immersion in ozone nanobubble water produces effects similar to those observed with UV irradiation. However, for future practical applications, ozone nanobubbles offer distinct advantages over UV irradiation. The samples in this study were SLA-treated Ti disks (titanium plates), but actual dental implant materials often have complex, screw-like geometries. Achieving uniform hydrophilicity on such intricate surfaces using UV irradiation is extremely challenging. In contrast, ozone nanobubble treatment enables uniform processing by simple immersion, even on surfaces with complex geometries. In our tests, hydrophobization of implant materials began to occur within 3 days after UV irradiation, whereas immersion in ozone nanobubble water maintained long-term superhydrophilicity, consistent with the results observed on Ti disks. Given that ozone nanobubble treatment can be applied regardless of the material's shape, it is expected to provide significant benefits not only for dental implants but also for other titanium-based medical devices.

■ ASSOCIATED CONTENT

Supporting Information

The Supporting Information is available free of charge at https://pubs.acs.org/doi/10.1021/acs.langmuir.4c03339.

UV−vis spectroscopy of the ozone nanobubble water, indicating a characteristic absorption peak corresponding to permanganate ions (MnO_4^-), and ESR spectrum of degraded ozone nanobubble water with the radical scavenger methanol (PDF)

https://doi.org/10.1021/acs.langmuir.4c03339
Langmuir XXXX, XXX, XXX−XXX

Video of the spread of a water droplet on a dry titanium disk that was immersed in ozone nanobubble water for 10 min and then dried with an air blower (MP4)

Video of the spread of a water droplet on a dry titanium disk that had been immersed in ozone nanobubble water for 10 min, dried with an air blower, and then left for 35 days before being tested (MP4)

Video of the spread of a water droplet on a dry titanium disk that was immersed in degraded ozone nanobubble water for 10 min and then dried with an air blower (MP4)

Video of the spread of a water droplet on a dry titanium disk that was immersed in a MnO_4^- solution for 10 min and then dried with an air blower (MP4)

AUTHOR INFORMATION

Corresponding Author

Masayoshi Takahashi − *New Industry Creation Hatchery Center, Tohoku University, Sendai, Miyagi 980-8579, Japan;* orcid.org/0000-0002-4984-5966; Phone: +81-22-795-3977; Email: masayoshi.takahashi.c1@tohoku.ac.jp

Authors

Masahiro Nakazawa − *Nakazawa Dental Clinic, Chiba 276-0033, Japan*

Takahiro Nishimoto − *Nanosui Company, Nippon Beatty Lease Company, Ltd., Shizuoka 416-0939, Japan*

Mitsuyuki Odajima − *Nikken Rentacom Company, Ltd., Tokyo 101-0064, Japan*

Yasuyuki Shirai − *New Industry Creation Hatchery Center, Tohoku University, Sendai, Miyagi 980-8579, Japan*

Shigetoshi Sugawa − *New Industry Creation Hatchery Center, Tohoku University, Sendai, Miyagi 980-8579, Japan*

Complete contact information is available at: https://pubs.acs.org/10.1021/acs.langmuir.4c03339

Notes

The authors declare no competing financial interest.

ACKNOWLEDGMENTS

The work was supported by the New Industry Creation Hatchery Center of Tohoku University and the Japan Science and Technology Agency (JPMJTM20K8).

REFERENCES

(1) Thiel, P. A.; Madey, T. E. The Interaction of Water with Solid Surfaces: Fundamental Aspects. *Surf. Sci. Rep.* **1987**, *7*, 211−385.

(2) Henderson, M. A. The Interaction of Water with Solid Surfaces: Fundamental Aspects Revisited. *Surf. Sci. Rep.* **2002**, *46*, 1.

(3) Yamamoto, S.; Andersson, K.; Bluhm, H.; Ketteler, G.; Starr, D. E.; Schiros, T.; Ogasawara, H.; Pettersson, L. G. M.; Salmeron, M.; Nilsson, A. Hydroxyl-Induced Wetting of Metals by Water at Near-Ambient Conditions. *J. Phys. Chem. C* **2007**, *111*, 7848−7850.

(4) Hodgson, A.; Haq, S. Water adsorption and the wetting of metal surfaces. *Surf. Sci. Rep.* **2009**, *64*, 381−451.

(5) Lausmaa, J.; Kasemo, B.; Mattsson, H. Surface spectroscopic characterization of titanium implant materials. *Appl. Surf. Sci.* **1990**, *44*, 133−146.

(6) Mouhyi, J.; Sennerby, L.; Pireaux, J.; Dourov, N.; Nammour, S.; Van Reck, J. An XPS and SEM evaluation of six chemical and physical techniques for cleaning of contaminated titanium implants. *Clin. Oral Implants Res.* **1998**, *9*, 185−194.

(7) Aita, H.; Hori, N.; Takeuchi, M.; Suzuki, T.; Yamada, M.; Anpo, M.; Ogawa, T. The effect of ultraviolet functionalization of titanium on integration with bone. *Biomaterials* **2009**, *30*, 1015−1025.

(8) Att, W.; Hori, N.; Takeuchi, M.; Ouyang, J.; Yang, Y.; Anpo, M.; Ogawa, T. Time-dependent degradation of titanium osteoconductivity: An implication of biological aging of implant materials. *Biomaterials* **2009**, *30*, 5352−5363.

(9) Rupp, F.; Gittens, R. A.; Scheideler, L.; Marmur, A.; Boyan, B. D.; Schwartz, Z.; Geis-Gerstorfer, J. A review on the wettability of dental implant surfaces I: Theoretical and experimental aspects. *Acta Biomaterialia* **2014**, *10*, 2894−2906.

(10) Gittens, R. A.; Scheideler, L.; Rupp, F.; Hyzy, S. L.; Geis-Gerstorfer, J.; Schwartz, Z.; Boyan, B. D. A review on the wettability of dental implant surfaces II: Biological and clinical aspects. *Acta Biomaterialia* **2014**, *10*, 2907−2918.

(11) Björneholm, O.; Hansen, M. H.; Hodgson, A.; Liu, L.-M.; Limmer, D. T.; Michaelides, A.; Pedevilla, P.; Rossmeisl, J.; Shen, H.; Tocci, G.; Tyrode, E.; Walz, M.-M.; Werner, J.; Bluhm, H. Water at Interfaces. *Chem. Rev.* **2016**, *116*, 7698−7726.

(12) Nakazawa, M.; Yamada, M.; Wakamura, M.; Egusa, H.; Sakurai, K. Activation of Osteoblastic Function on Titanium Surface with Titanium-Doped Hydroxyapatite Nanoparticle Coating: An In Vitro Study. *Int. J. Oral Maxillofac Implants* **2017**, *32*, 779−791.

(13) Gentleman, M. M.; Ruud, J. A. Role of Hydroxyls in Oxide Wettability. *Langmuir* **2010**, *26*, 1408−1411.

(14) Metiu, H.; Chrétien, S.; Hu, Z.; Li, B.; Sun, X. Y. Chemistry of Lewis Acid−Base Pairs on Oxide Surfaces. *J. Phys. Chem. C* **2012**, *116*, 10439−10450.

(15) Agarwal, A.; Ng, W. J.; Liu, Y. Principle and applications of microbubble and nanobubble technology for water treatment. *Chemosphere* **2011**, *84*, 1175−1180.

(16) Tsuge, H. *Micro- and Nanobubbles*; Fundamentals and Applications; CRC Press: Boca Raton, FL, 2014; pp 307−352.

(17) Alheshibri, M.; Qian, J.; Jehannin, M.; Craig, V. S. J. A History of Nanobubbles. *Langmuir* **2016**, *32*, 11086−11100.

(18) Azevedo, A.; Etchepare, R.; Calgaroto, S.; Rubio, J. Aqueous dispersions of nanobubbles: Generation, properties and features. *Minerals Eng.* **2016**, *94*, 29−37.

(19) Bunkin, N. F.; Shkirin, A. V.; Suyazov, N. V.; Babenko, V. A.; Sychev, A. A.; Penkov, N. V.; Belosludtsev, K. N.; Gudkov, S. V. Formation and Dynamics of Ion-Stabilized Gas Nanobubble Phase in the Bulk of Aqueous NaCl Solutions. *J. Phys. Chem. B* **2016**, *120*, 1291−1303.

(20) Oh, S. H.; Kim, J. M. Generation and Stability of Bulk Nanobubbles. *Langmuir* **2017**, *33*, 3818−3823.

(21) Wang, L.; Miao, X.; Ali, J.; Lyu, T.; Pan, G. Quantification of Oxygen Nanobubbles in Particulate Matters and Potential Applications in Remediation of Anaerobic Environment. *ACS Omega* **2018**, *3*, 10624−10630.

(22) Alheshibri, M.; Craig, V. S. J. Differentiating between Nanoparticles and Nanobubbles by Evaluation of the Compressibility and Density of Nanoparticles. *J. Phys. Chem. C* **2018**, *122*, 21998−22007.

(23) Nirmalkar, N.; Pacek, A. W.; Barigou, M. On the Existence and Stability of Bulk Nanobubbles. *Langmuir* **2018**, *34*, 10964−10973.

(24) Rak, D.; Ovadová, M.; Sedlák, M. (Non)Existence of Bulk Nanobubbles: The Role of Ultrasonic Cavitation and Organic Solutes in Water. *J. Phys. Chem. Lett.* **2019**, *10*, 4215−4221.

(25) Ke, S.; Xiao, W.; Quan, N.; Dong, Y.; Zhang, L.; Hu, J. Formation and Stability of Bulk Nanobubbles in Different Solutions. *Langmuir* **2019**, *35*, 5250−5256.

(26) Jadhav, A. J.; Barigou, M. Bulk Nanobubbles or Not Nanobubbles: That is the Question. *Langmuir* **2020**, *36*, 1699−1708.

(27) Rak, D.; Sedlák, M. Comment on "Bulk Nanobubbles or Not Nanobubbles: That is the Question". *Langmuir* **2020**, *36*, 15618−15621.

(28) Li, P.; Wang, J.; Liao, Z.; Ueda, Y.; Yoshikawa, K.; Zhang, G. Microbubbles for Effective Cleaning of Metal Surfaces Without Chemical Agents. *Langmuir* **2022**, *38*, 769−776.

(29) Takahashi, M.; Ishikawa, H.; Asano, T.; Horibe, H. Effect of Microbubbles on Ozonized Water for Photoresist Removal. *J. Phys. Chem. C* **2012**, *116*, 12578−12583.
(30) Takahashi, M.; Chiba, K.; Li, P. Formation of Hydroxyl Radicals by Collapsing Ozone Microbubbles under Strongly Acidic Conditions. *J. Phys. Chem. B* **2007**, *111*, 11443−11446.
(31) Li, P.; Takahashi, M.; Chiba, K. Degradation of phenol by the collapse of microbubbles. *Chemosphere* **2009**, *75*, 1371−1375.
(32) Li, P.; Takahashi, M.; Chiba, K. Enhanced free-radical generation by shrinking microbubbles using a copper catalyst. *Chemosphere* **2009**, *77*, 1157−1160.
(33) Takahashi, M.; Nakatsuka, R.; Kutsuna, S.; Shirai, Y.; Sugawa, S. Mineralization of Poly(vinyl alcohol) by Ozone Microbubbles under a Wide Range of pH Conditions. *Langmuir* **2023**, *39*, 15215−15221.
(34) Takahashi, M.; Shirai, Y.; Sugawa, S. Free-Radical Generation from Bulk Nanobubbles in Aqueous Electrolyte Solutions: ESR Spin-Trap Observation of Microbubble-Treated Water. *Langmuir* **2021**, *37*, 5005−5011.
(35) Takahashi, M.; Shirai, Y.; Sugawa, S. Nanoshell Formation at the Electrically Charged Gas−Water Interface of Collapsing Microbubbles: Insights from Atomic Force Microscopy Imaging. *J. Phys. Chem. Lett.* **2024**, *15*, 220−225.
(36) Takahashi, M.; Kawamura, T.; Yamamoto, Y.; Ohnari, H.; Himuro, S.; Shakutsui, H. Effect of Shrinking Microbubble on Gas Hydrate Formation. *J. Phys. Chem. B* **2003**, *107*, 2171−2173.
(37) Takahashi, M. ζ Potential of Microbubbles in Aqueous Solutions: Electrical Properties of the Gas−Water Interface. *Phys. Chem. B* **2005**, *109*, 21858−21864.
(38) Takahashi, M.; Chiba, K.; Li, P. Free-Radical Generation from Collapsing Microbubbles in the Absence of a Dynamic Stimulus. *J. Phys. Chem. B* **2007**, *111*, 1343−1347.
(39) Lausmaa, J.; Kasemo, B.; Mattsson, H. Surface spectroscopic characterization of titanium implant materials. *Appl. Surf. Sci.* **1990**, *44*, 133−146.
(40) Hanawa, T. Titanium−Tissue Interface Reaction and Its Control with Surface Treatment. *Front. Bioeng. Biotechnol.* **2019**, *7*, 170.
(41) Kim, M.; Shoji, A.; Kobayashi, T.; Shirai, Y.; Sugawa, S.; Takahashi, M. Accelerated germination of aged recalcitrant seeds by K^+-rich bulk oxygen nanobubbles. *Sci. Rep.* **2023**, *13*, 3301.
(42) Sofyana, N. T.; Refli, R.; Takahashi, M.; Sakamoto, K. Oxygen nanobubble water affects wound healing of fibroblast WI-38 cells Get access Arrow. *Biosci., Biotechnol., Biochem.* **2023**, *87*, 620−626.
(43) Mori, K.; Hayashi, Y.; Akiba, T.; Noguchi, Y.; Yoshida, Y.; Kai, A.; Yamada, S.; Sakai, S.; Hara, M. Effects of Hand Hygiene on Feline Calicivirus Inactivation and Removal as Norovirus Surrogate Treated with Antiseptic Hand Rubbing, Wet Wipes, and Functional Water. *Jpn. J. Infect. Dis.* **2007**, *81*, 249−255.
(44) Hayakumo, S.; Arakawa, S.; Takahashi, M.; Kondo, K.; Mano, Y.; Izumi, Y. Effects of ozone nano-bubble water on periodontopathic bacteria and oral cells - in vitro studies. *Sci. Technol. Adv. Mater.* **2014**, *15*, No. 055003.
(45) Fujishima, A.; Rao, T. N.; Tryk, D. A. Titanium dioxide photocatalysis. *Journal of istry and ogy C: Photochemistry Reviews, J. Photochem. Photobiol. C-Photochem. Rev.* **2000**, *1*, 1−21.
(46) Hashimoto, K.; Irie, H.; Fujishima, A. TiO2 photocatalysis: a historical overview and future prospects. *Jpn. J. Appl. Phys.* **2005**, *44*, 8269−8285.
(47) Chowdhury, S. S.; Pandey, P. R.; Kumar, R.; Roy, S. Effect of shape of protrusions and roughness on the hydrophilicity of a surface. *Chem. Phys. Lett.* **2017**, *685*, 34−39.

https://doi.org/10.1021/acs.langmuir.4c03339
Langmuir XXXX, XXX, XXX−XXX